RSC Advances

PAPER

View Article Online
View Journal | View Issue

Cite this: *RSC Adv.*, 2017, **7**, 12455

Design, synthesis, and biological evaluation of oxazolidone derivatives as highly potent *N*-acylethanolamine acid amidase (NAAA) inhibitors†

Jie Ren,[a] Yuhang Li,*[ab] Hongwei Ke,[c] Yanting Li,[a] Longhe Yang,[d] Helin Yu,[a] Rui Huang,[a] Canzhong Lu[b] and Yan Qiu*[a]

Received 27th December 2016
Accepted 16th February 2017

DOI: 10.1039/c6ra28734d

rsc.li/rsc-advances

N-Acylethanolamine-hydrolyzing acid amidase (NAAA) is a lysosomal enzyme that catalyzes the hydrolysis of endogenous fatty acid ethanolamides (FAEs), such as *N*-palmitoylethanolamide (PEA). PEA exhibits anti-inflammatory and analgesic activities by engaging peroxisome proliferator-activated receptor α (PPAR-α). Preventing PEA degradation by inhibition of NAAA has been proposed as a novel strategy for the treatment of inflammation and pain. In the present study, we reported the discovery of the oxazolidone derivative as a novel scaffold for NAAA inhibitors, and studied the structure–activity relationship (SAR) by modification of the side chain and terminal lipophilic substituents. The results showed that the link chain length of C5, straight and saturated linkages were the preferred shape patterns for NAAA inhibition. Several nanomolar NAAA inhibitors were described, including **2f**, **3h**, **3i** and **3j** with IC_{50} values of 270 nM, 150 nM, 100 nM and 190 nM, respectively. Enzymatic degradation studies suggested that **2f** inhibited NAAA in a selective, noncompetitive and reversible pattern. Moreover, **2f** showed high anti-inflammatory and analgesic activities after systemic and oral administration.

1 Introduction

N-Acylethanolamine-hydrolyzing acid amidase (NAAA) is a lysosomal cysteine hydrolase widely expressed in many tissues, especially those associated with immune responses, such as the lungs, spleen, and small intestine. NAAA participates in the control of inflammatory and pain[1] *via* involving in the hydrolysis of endogenous palmitoylethanolamide (PEA). PEA is a multifunctional lipid mediator that has been shown to inhibit peripheral inflammation[2–4] and cell degranulation, and exhibits anti-nociceptive activities in rat and mouse models of acute and chronic pain.[5–7] Moreover, PEA also could alleviate skin inflammation[8] and neuropathic pain in humans.[9] Those effects are mainly attribute to the ability of PEA to engage nuclear receptor peroxisome proliferator-activated receptor-alpha (PPAR-α). In recent years, PEA has attracted increasing attention because of its potential therapeutic effects in inflammation and pain. Preventing PEA degradation by inhibition of NAAA[10] may provide a novel strategy for the treatment of inflammatory and pain.[4,11] For this reason, NAAA has been pursued as a potential drug target.

Despite the increasing interest in the design of NAAA inhibitors as anti-inflammatory and analgesic agents, only few potent NAAA inhibitors have been identified so far.[12,13] There are two main categories of NAAA inhibitors reported, irreversible covalent inhibitors, such as β-lactone derivatives[14–18] and non-covalent reversible inhibitors, such as benzothiazole-piperazine derivatives.[19] Although covalent inhibitors, such as **(*S*)-OOPP**,[4] ARN077,[11] ARN726 (ref. 20) (Fig. 1) demonstrated profound anti-inflammatory effects in several animal models, their application is limited due to the poor chemical and plasma stability. These compounds degraded in phosphate buffered saline (PBS) within 120 min and were rapidly cleaved in plasma.[16] Non-covalent reversible inhibitors, such as, benzothiazole-piperazine derivatives (Fig. 1),[19] are selective, reversible, and competitive NAAA inhibitors. However, only few potent reversible NAAA inhibitors with drug-like properties have been identified so far. Highly potent, stable and reversible NAAA inhibitors are still highly desired for the treatment of inflammation and pain.

In our previous study, we designed pyrrolidine-based derivatives **1a** and **1b** (Fig. 1)[21] as NAAA inhibitors. Substitution of the saturated alkyl chain of **1a** with an aryl-containing lipophilic moiety leaded to a potent NAAA inhibitor **1b** (IC_{50} = 2.1 μM). *In vivo* pharmacological studies indicated that **1b** reduced the mRNA expression levels of inducible nitric oxide synthase and

[a]*Medical College, Xiamen University, Xiamen, Fujian 361102, P. R. China. E-mail: yuhangli@fjirsm.ac.cn; yanqiu@xmu.edu.cn*

[b]*Xiamen Institute of Rare-earth Materials, Haixi Institutes, Chinese Academy of Sciences, Fujian 361005, P. R. China*

[c]*College of Ocean and Earth Science, Xiamen University, Xiamen, Fujian, 361005, P. R. China*

[d]*Engineering Research Center of Marine Biological Resource Comprehensive Utilization, Third Institute of Oceanography, State Oceanic Administration, Xiamen 361005, P. R. China*

† Electronic supplementary information (ESI) available: Full experimental details, characterization, and ^{1}H-NMR and ^{13}C-NMR spectra of the intermediate and final compounds. See DOI: 10.1039/c6ra28734d

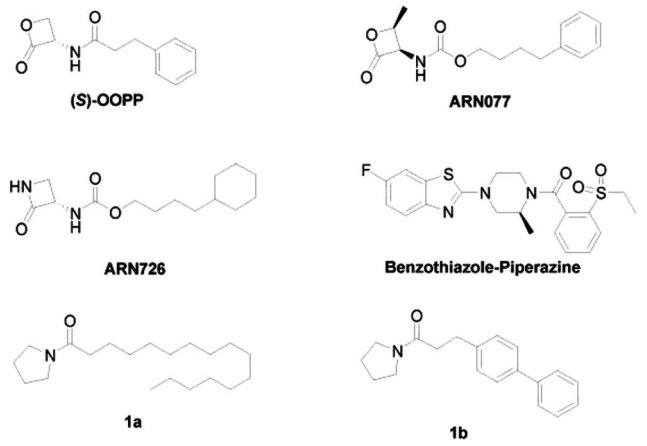

Fig. 1 The chemical structures of classic NAAA inhibitors.

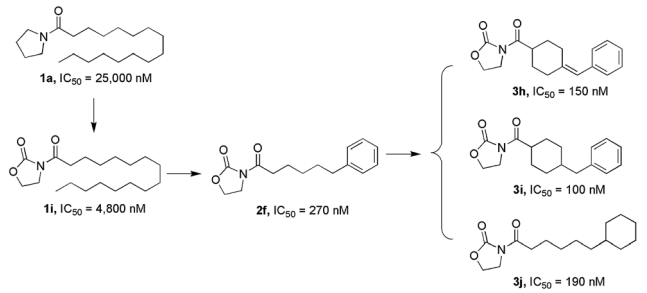

Fig. 2 Design strategy for oxazolidone derivatives as NAAA inhibitors.

interleukin-6, as well as increased the intracellular PEA levels in mouse macrophages with lipopolysaccharide-induced inflammation.[21] Moreover, **1b** exhibited excellent chemical stability and plasma stability ($t_{\frac{1}{2}} > 16$ h).

In the present study, we further modified **1a** to obtain more potent and biologically stable NAAA inhibitors. A nanomolar NAAA inhibitor **2f** was discovered (IC_{50} = 270 nM), which exerted profound anti-inflammatory and anti-nociceptive effects in rats.[22] We then carried out structure–activity relationship (SAR) studies on **2f** by modification of the pyrrolidine ring and the lipophilic chain, which led to the identification of several more potent nanomolar NAAA inhibitors, such as **3h**, **3i** and **3j** (Fig. 2). Compound **2f** was then selected as a model molecule to study the NAAA inhibition mechanisms and *in vivo* anti-inflammatory and analgesic activities of oxazolidone derivatives. The results showed that **2f** inhibited NAAA in a selective and highly reversible pattern, and efficiently reduced inflammatory and pain after systemic and oral administration. Oral administration of **2f** (30 mg kg^{-1}) exhibited the same efficacy with commercial nonsteroidal anti-inflammatory drug ibuprofen at a 6.7-fold higher dose (200 mg kg^{-1}).

2 Results and discussion

2.1 Synthesis of oxazolidone derivatives

First, we synthesized a series of oxazolidone derivatives with different side chains and terminal lipophilic substituents. Compounds **1a**, **1j–1o**, and **1q–1t** were prepared by the amidation of palmitoyl chloride with the corresponding amine in the presence of triethylamine (Scheme 1).[21] **1l** and **1m** were prepared by the methylation of **1q** and **1r** with iodomethane in the presence of sodium hydride, respectively (Scheme 2).[23] **1p** was prepared by Dess–Martin periodinane oxidation of **1j** or **1k** (Scheme 3).[24] **1c** and **1d** were prepared by the acidic deprotection of pyrrolidine derivatives **1c-1** and **1d-1**, which were obtained by the amidation of (*R*)- or (*S*)-3-(*tert*-butoxycarbonylamino)pyrrolidine with palmitoyl chloride, respectively (Scheme 4).[25,26] **1e** and **1f** were synthesized by a two-step reaction starting from **1q** and **1r**, which were converted to iodide derivatives by I_2 and PPh_3, respectively, followed by hydrogenation with H_2 (Scheme 5).[27,28] **1g**, **2a–2h**, **3a–3d** and **3k–3s** were synthesized by the imidate reaction, employing the corresponding acyl chloride with 2-pyrrolidone, 2-imidazolidone, or 2-oxazolidone in the presence of *n*-BuLi, respectively (Scheme 6).[29] **3e–3g** were synthesized by the amidation of 2-oxooxazolidine-3-carbonyl chloride, generated by reaction of 2-oxazolidone and bis(trichloromethyl) carbonate, with the corresponding substituted piperazine or piperidine (Scheme 7).[30] HPLC analysis indicated >99% purity for compound **1g**, **1e–1i**, **2b**, **2d**, **2f–2h**, **3c**, **3e**, and **3g**, >98% purity for **1c–1d**, **1f**, **2a**, **2e**, **3a**, **3b** and **3g–3i**, and >97% purity for **2c** and **3d** (Table S3†).

2.2 NAAA inhibition by oxazolidone derivatives

The NAAA inhibition capability of these newly synthesized compounds were tested using heptadecenoylethanolamide as a substrate. Since many NAAA inhibitors also block fatty acid amide hydrolase (FAAH), the FAAH inhibition of these compounds also was examined to obtain NAAA selective inhibitors. **(*S*)-OOPP** and well known FAAH inhibitor **URB597** were used as standard compounds in the enzymatic assay. The results showed that substitution at 3-position of pyrrolidine with an amino group (**1c**, **1d**) slightly increased NAAA and FAAH

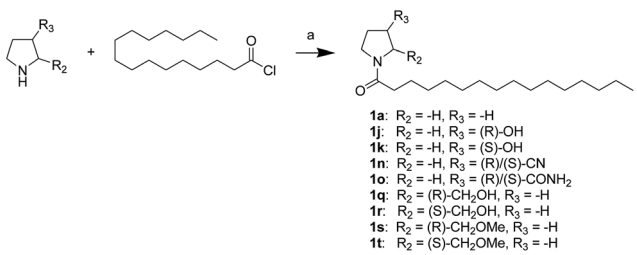

Scheme 1 The synthesis of compounds **1a**, **1j**, **1k**, **1n**, **1o**, and **1q–1t**. Reagents and conditions: (a) Et_3N, CH_2Cl_2, room temperature.

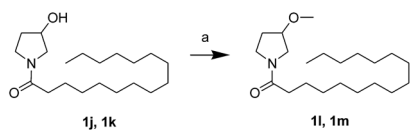

Scheme 2 The synthesis of compounds **1l** and **1m**. Reagents and conditions: (a) NaH, MeI, tetrahydrofuran (THF), 0 °C.

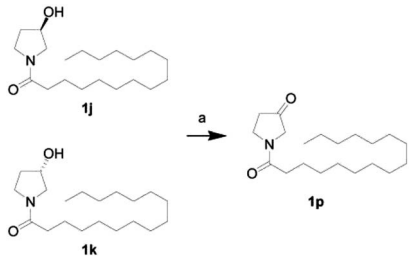

Scheme 3 The synthesis of compound **1p**. Reagents and conditions: (a) Dess–Martin periodinane, CH_2Cl_2, room temperature.

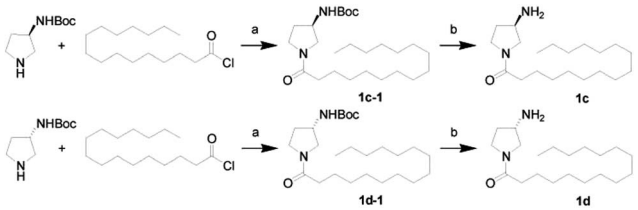

Scheme 4 The synthesis of compounds **1c** and **1d**. Reagents and conditions: (a) Et_3N, CH_2Cl_2, room temperature; (b) HCl, dioxane, 0 °C.

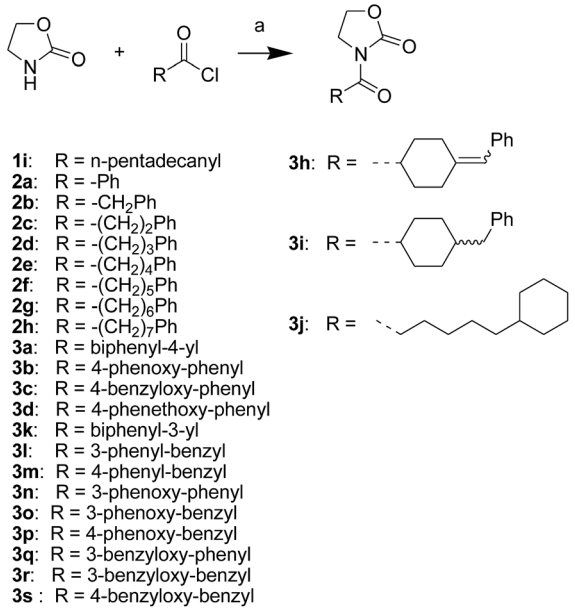

Scheme 6 The synthesis of compounds **1i**, **2a–2h**, **3a–3d** and **3h–3s**. Reagents and conditions: (a) *n*-BuLi, THF, −78 °C.

inhibition, and substitutions at the 2-position with (*S*)-methyl (**1f**) or carbonyl (**1g**) slightly or moderately enhanced inhibition towards NAAA without changing inhibition against FAAH. However, (*R*)-methyl (**1e**), hydroxy (**1j**, **1k**), methoxy (**1l**, **1m**), cyano (**1n**), formamide (**1o**), hydroxymethyl (**1q**, **1r**) and methoxymethyl (**1s**, **1t**) substituents diminished the NAAA and FAAH inhibitory effects (Table S1†). **1g** exhibited low-micromolar inhibition on NAAA activity (IC_{50} = 4.6 ± 0.48 μM), and it was over 5-fold more potent towards NAAA than FAAH (Table 1). To further optimize the hydrophilic moieties, a series of **1g** isosteres were synthesized and tested (**1h**, **1i**) (Table 2). Enzymatic assay results showed that **1i** with oxazolidone ring had similar effects on NAAA inhibition as **1g**, but **1i** exhibited dramatically enhanced selectivity towards NAAA. Less than 10% FAAH activity was inhibited by **1i** even at a concentration of 100 μM. Therefore, 2-oxazolidone ring was selected as the template for further optimization.

It has been reported that substitutions of the saturated alkyl chain with aryl-containing lipophilic moieties could enhance the inhibitory potency on NAAA and improved the drug-like properties.[14,21] Therefore, a series of oxazolidone derivatives incorporating a phenyl ring at the terminus were synthesized and tested. As shown in Table 3, **2a** with the chain length of C0 exhibited low-micromolar inhibitory potency toward NAAA (IC_{50} = 3.4 ± 0.42 μM), while **2f** with the chain length of C5 exhibited excellent potency (IC_{50} = 0.27 ± 0.04 μM), 3-fold more potent than (***S*)-OOPP** tested under the same experimental conditions. Interestingly, sharply reduced or even abolished activity was observed as the chain length decreased from C5 to C1 or increased from C5 to C7. We are not quite sure why their potency dramatically changed when we varied the link chain length, probably because these oxazolidone imides with different chain length are activated to different extent when contacting the NAAA.

To further optimize the NAAA inhibition activity of **2f**, we replaced the rotatable bond of the acyl chain of **2f** with an additional phenyl group. As shown in Table 4 and S2,† a series of analogs corresponding to biphenyl (**3a**, **3k–3m**), phenoxyphenyl

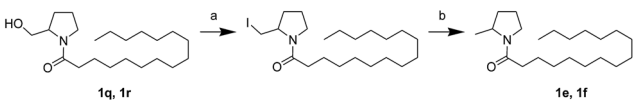

Scheme 5 The synthesis of compounds **1e** and **1f**. Reagents and conditions: (a) PPH_3, I_2, THF, room temperature; (b) H_2, Pd/C, CH_3OH, room temperature.

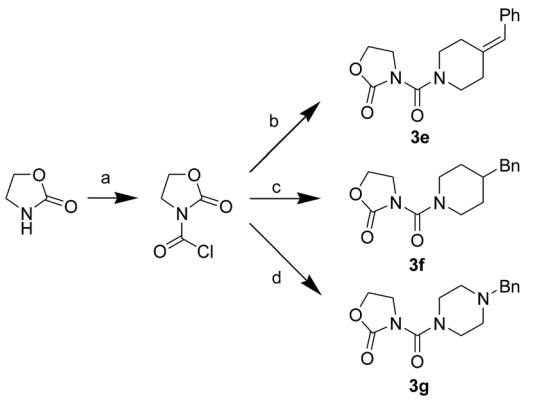

Scheme 7 The synthesis of compounds **3e–3g**. Reagents and conditions: (a) bis(trichloromethyl) carbonate, Et_3N, CH_2Cl_2, room temperature; (b) 4-benzylidenepiperidine, CH_2Cl_2, room temperature; (c) 4-benzylpiperidine, CH_2Cl_2, room temperature; (d) 1-benzylpiperazine, CH_2Cl_2, room temperature.

Table 1 Inhibitory effects of compounds **1a–1g**, (*S*)-OOPP and URB597 on NAAA and FAAH activities

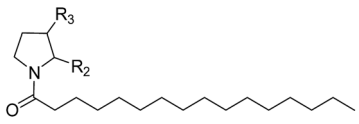

Compound	R_2	R_3	IC_{50} of NAAA (μM)	IC_{50} of FAAH (μM)
1a	–H	–H	25 ± 5.7	21 ± 4.5
1c	–H	(*R*)-NH_2	10 ± 0.95	3.5 ± 0.65
1d	–H	(*S*)-NH_2	11 ± 1.2	4.0 ± 0.81
1e	(*R*)-Me	–H	>100	28 ± 2.7
1f	(*S*)-Me	–H	15 ± 2.3	18 ± 3.2
1g	=O	–H	4.6 ± 0.48	25 ± 5.3
(*S*)-OOPP			0.83 ± 0.1	>20
URB597			>100	0.026 ± 0.005

(**3b**, **3n–3p**), and benzyloxyphenyl (**3c**, **3q–3s**) were obtained and examined. Compared to **2a**, 1,4-substituted phenoxyphenyl (**3b**, IC_{50} = 0.68 ± 0.11 μM) and benzyloxyphenyl (**3c**, IC_{50} = 2.3 ± 0.36 μM) analogs were approximately 10-fold and 2-fold more potent. However, 1,4-substituted bipheny analog **3a** (IC_{50} = 9.4 ± 1.2 μM) was 2-fold less potent (Table 4), and 1,3-substituted isomers (**3k**, **3l**, **3n**, **3o**, **3q**, **3r**) were completely inert for NAAA inhibition (Table S2†). The results indicated that straight structures are preferred shape for the hydrophobic channel of NAAA, which is in agreement with previous reports.[14,17] The binding pocket of NAAA proximal to the carbonyl moieties seemed to be narrow, as such, only a phenyl moiety is tolerated at this region. Therefore, incorporation of an extra methylene group between the biaryl and carbonyl groups (**3m**, **3p** and **3s**) significantly decreased NAAA inhibition.

It's worth noting that the position of the terminal phenyl groups in biaryl series compounds (**3a–3d**) is corresponding to the location of phenyl moieties in the phenylalkyl series compounds (**2e–2h**). Increasing the length of the terminal aryl group of **3a** by insertion of an oxygen atom or a methyleneoxy unit between the phenyl rings led to 14-fold (**3b**) or 4-fold (**3c**) higher potency, whereas the insertion of an additional methylene unit to the aliphatic linker of **3c** significantly decreased activity (**3d**). These results highlighted the importance of the optimal length and connecting pattern of the aryl-containing lipophilic moieties.

Table 2 Inhibitory effects of compounds **1h–1j** on NAAA and FAAH activities

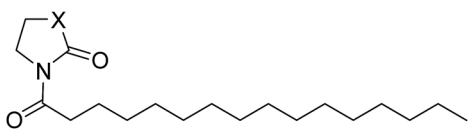

Compound	X	IC_{50} of NAAA (μM)	IC_{50} of FAAH (μM)
1g	C	4.6 ± 0.48	25 ± 5.3
1h	NH	>100	27 ± 4.9
1i	O	**4.8 ± 0.63**	**>100**

Table 3 Inhibitory effects of compounds **2a–2h** on NAAA and FAAH activities

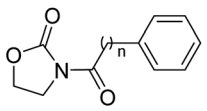

Compound	*n*	IC_{50} of NAAA (μM)	IC_{50} of FAAH (μM)
2a	0	3.4 ± 0.42	>20
2b	1	>20	>20
2c	2	>20	>20
2d	3	12.4 ± 2.0	>20
2e	4	8.3 ± 1.8	>20
2f	5	**0.27 ± 0.04**	>20
2g	6	6.3 ± 1.2	>20
2h	7	>20	>20

It has been reported that NAAA prefer saturated substrates *e.g.*, *N*-myristoylethanolamine and PEA, rather than unsaturated substrates, *e.g.*, AEA.[1] Therefore, we studied whether the replacement of a phenyl ring with a 6-member ring can improve the NAAA inhibition. A series of additional derivatives of **2f** were then synthesized and examined (Table 5). The results showed that introducing hexane ring further enhanced the NAAA inhibitory potency. We found two highly potent NAAA inhibitors **3h** and **3i** with a IC_{50} value of 150 nM and 100 nM, respectively, around 2-fold more potent than **2f**. Moreover, saturated linkages were found to be more beneficial for the activity than unsaturated benzene ring (**3h**, **3i** *vs.* **3a–3c**; **3j** *vs.* **2f**). However, nitrogen atoms substitution of the saturated hexane significantly reduced the activity (**3e–3g**).

2.3 NAAA inhibition pattern

To further understand the NAAA inhibition pattern of these oxazolidone derivatives, compound **2f** was selected as a model

Table 4 Inhibitory effects of compounds **3a–3d** on NAAA and FAAH activities

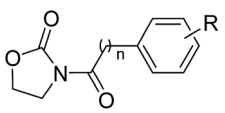

Compound	*n*	R	IC_{50} of NAAA (μM)	IC_{50} of FAAH (μM)
3a	0	4-Ph	9.4 ± 1.2	>20
3b	0	4-OPh	**0.68 ± 0.11**	>20
3c	0	4-OBn	2.4 ± 0.36	>20
3d	0	4-OCH_2CH_2Ph	>20	>20

Table 5 Inhibitory effects of compounds **3e–3j** on NAAA and FAAH activities

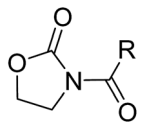

Compound	R	IC_{50} of NAAA (μM)	IC_{50} of FAAH (μM)
3e	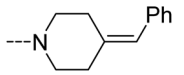	>20	>20
3f	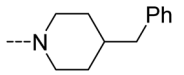	>20	15.3 ± 2.4
3g	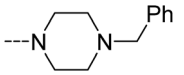	>20	21.2 ± 4.2
3h	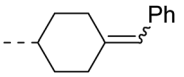	**0.15 ± 0.03**	>20
3i	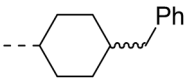	**0.10 ± 0.03**	>20
3j	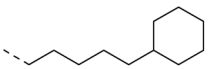	**0.19 ± 0.02**	>20

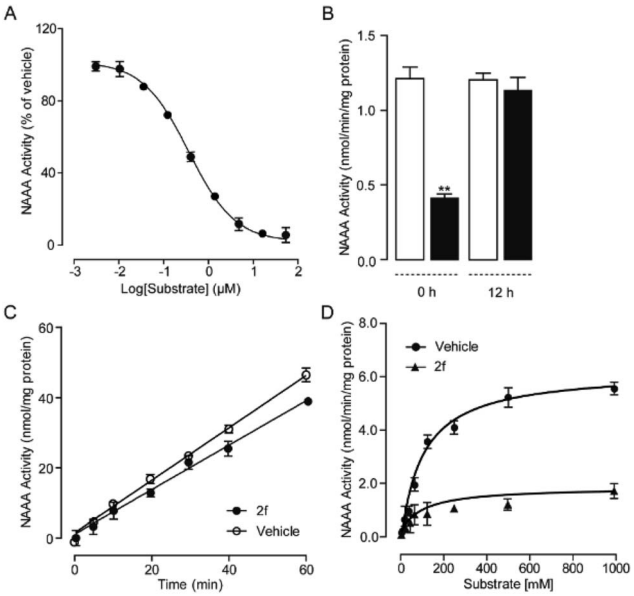

Fig. 3 Characterization of **2f** as a reversible and noncompetitive NAAA inhibitor. (A) Concentration-dependent inhibitory effect of **2f** on the rat NAAA. (B) NAAA activity in the presence of vehicle (open columns) or **2f** (closed columns) before and 12 h after dialysis. ** $P < 0.01$ *vs.* vehicle, $n = 3$; (C) rapid dilution NAAA assay in the presence of vehicle (1% DMSO, open circles) or **2f** (closed circles). (D) Michaelis–Menten analysis of the NAAA reaction in the presence of vehicle (1% DMSO, closed circles) and **2f** (0.5 μM, triangles).

molecule and its interaction mode with NAAA protein in cells was studied. The results showed that **2f** displayed a profound inhibition toward recombinant human NAAA (IC_{50} = 0.27 ± 0.04 μM, Fig. S1A†) and recombinant rat NAAA in NAAA-transfected HEK293 cells (IC_{50} = 0.42 ± 0.04 μM, Fig. S1B†), which were similar to the data obtained with the NAAA protein extract. Dialysis (Fig. 3B) and rapid dilution (Fig. 3C) of the **2f**–NAAA interaction complex almost completely restored the NAAA activity. Moreover, Michaelis–Menten kinetic analysis revealed that **2f** induced changes in the maximal catalytic velocity (V_{max}) of NAAA (V_{max} in nmol per min per mg protein, vehicle: 6.0 ± 0.51; and **2f**, 0.3 μM: 1.9 ± 0.15, Fig. 3D) but did not affect Michaelis–Menten constant K_m (K_m in μM, vehicle: 174 ± 26; and **2f**, 0.3 μM: 212 ± 24). These results indicated that **2f** is a reversible and noncompetitive NAAA inhibitor.

2.4 *In vivo* anti-inflammatory and analgesic activities of 2f

Finally, the *in vivo* anti-inflammation and analgesic activities of **2f** was studied in different pain and inflammation mice models. Experimental mice were treated with **2f** *via* intraperitoneal injection or intragastrical administration. The behavioural response of Mice to formalin stimulation was divided to the first-phase of acute pain (0–10 min) and the second-phase of chronic pain (15–35 min). Single treatment of **2f** (10 mg kg^{-1}, i.p.) decreased second-phase but not first-phase (Fig. 4), suggesting a central mechanism of action of **2f**. The reduced licking time by **2f** at the second-phase was reversed by PPAR-α antagonist MK886 (2 mg kg^{-1}, i.p.), which indicated that **2f** relieve pain in a PPAR-α dependent pathway.

The anti-inflammatory activity of **2f** was tested in 12-*o*-tetradecanoylphorbol-13-acetate (TPA) induced mice ear edema model. A commercial nonsteroidal anti-inflammatory drug, ibuprofen (200 mg kg^{-1}) was intragastrically administrated as a positive control. The results showed that intragastrical administration of **2f** (30, 100 mg kg^{-1}) significantly reduce ears edema. Oral administration of compound **2f** (30 mg kg^{-1}) presented the same efficacy with ibuprofen (200 mg kg^{-1}). Moreover, **2f** significantly prevent the production of proinflammatory cytokines, including TNF-α, IL-6, COX-2 and NF-κB in mRNA level (Fig. 5).

For many nonsteroidal anti-inflammatory drugs, such as COX-2 inhibitors, adverse gastrointestinal effects and increased cardiovascular risks are two main limitations for their clinical application. We tested the toxicity of **2f** by monitoring its influence on food intake, body weight and ether-a-go-go-related-gene (hERG) channel activity. Long-term studies suggested that intragastrical administration of **2f** (30 mg kg^{-1} for 30 days, 100 mg kg^{-1} for 10 days) had no significant effects on food intake and body weight in mice (Fig. S2†). Mice stomach anatomy indicated that **2f** did not cause gastrointestinal hemorrhages, while indomethacin (20 mg kg^{-1} for 3 days, ig) resulted in obvious hemorrhages (Fig. S3†). The low gastrointestinal side effects of **2f** may be because it induces analgesia and anti-inflammatory *via* enhancement of PEA rather than reducing prostaglandins (PGs) in the gut. Moreover, the activity of hERG channels in CHO cells was only inhibited by 38.3% by

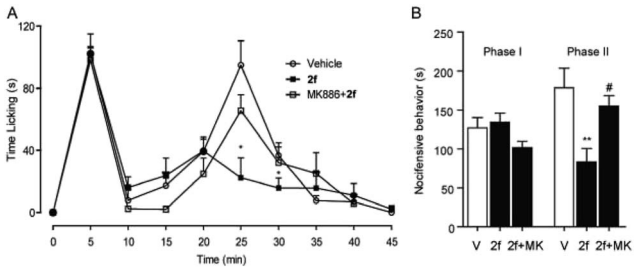

Fig. 4 2f attenuated formalin-induced pain behaviors. (A) 2f (10 mg kg^{-1}, i.p., open squares), injected 45 min prior to formalin treatment, produced time-dependent changes in composite pain score relative to vehicle (5% PEG/5% Tween-80 in saline, 10 mL kg^{-1}, i.p., open cycles), or a combination of 2f and PPAR-α antagonist MK886 (2 mg kg^{-1}, i.p., close squares). * $P < 0.1$ *vs.* vehicle; (B) 2f (close bar) reduced the licking time during phase 2 of the formalin response, ** $P < 0.1$ *vs.* vehicle (open bar). MK886 (2 mg kg^{-1}, i.p., close bar) prevented the anti-nociceptive effects of F96, # $P < 0.1$ *vs.* 2f. V represents vehicle (5% PEG/5% Tween-80 in saline), and MK represents PPAR-α antagonist MK 886.

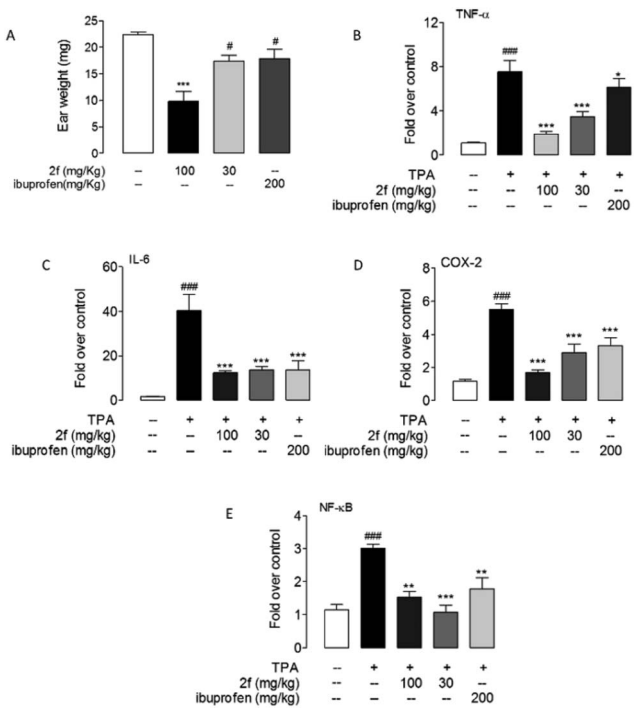

Fig. 5 Compound 2f alleviated TPA-induced inflammation. Effects of oral administration of 2f and ibuprofen on mice ears edema (A) and mRNA expression levels of TNF-α (B), IL-6 (C), COX-2 (D) and NF-κB (E) in mice ear treated with vehicle (open bars) or TPA (closed bars). Vehicle, 0.1% DMSO; TPA, 0.03% in acetone. ### $P < 0.001$ *vs.* vehicle; * $P < 0.1$, ** $P < 0.01$, *** $P < 0.001$ *vs.* TPA control, $n = 8$–10.

40 μM 2f (Fig. S4†), a concentration far above its threshold for NAAA inhibition. However, cisapride, a COX-2 inhibitor, inhibited 50% hERG at a concentration of 0.1 μM. These results suggested that with lower gastrointestinal and cardiovascular side effects, oxazolidone derivatives are promising anti-inflammatory drug candidates in clinical translation.

3 Conclusion

In conclusion, we report the discovery of oxazolidone derivatives as a novel scaffold of NAAA inhibitors. The NAAA inhibition activity of oxazolidone derivatives was modulated by the side chain and terminal lipophilic substituents. The results showed that the link chain length of C5, straight and saturated linkages were the preferred shape patterns. Several nanomolar NAAA inhibitors (**2f**, **3b**, **3h**, **3i** and **3j**) were developed. Compound **2f** exhibited highly potent and selective inhibitory activity towards NAAA *via* a competitive and reversible pattern. Moreover, *in vivo* study showed that **2f** had significant anti-inflammatory and analgesic effects with low side effects. Our study demonstrated that oxazolidone derivatives is a class of potent NAAA inhibitors holds great promise for clinical translation. We anticipate that these oxazolidone derivatives will help better understand the function of NAAA and facilitate the development of improved therapies for inflammation and pain.

4 Materials and methods

4.1 Materials and instruments

All reagents used in the present study were purchased from Sigma-Aldrich (Shanghai, China) unless otherwise indicated. Tetrahydrofuran was distilled prior to use from sodium benzophenone ketyl. Dichloromethane (CH_2Cl_2) was distilled from phosphorus pentoxide. Dimethylformamide (DMF) was distilled from calcium hydride. Silica gel (300–400 mesh) from Yantai Athy Chemical Technology Co. Ltd. (Zhifu, China) was used for column chromatography, and compounds were eluted with an ethyl acetate/petroleum ether (PE) (60–90 °C) mixture (unless otherwise stated).

The ^{1}H-NMR and ^{13}C-NMR spectra were recorded on a Bruker 400 spectrometer (400 MHz for ^{1}H, 100 MHz for ^{13}C), using $CDCl_3$, d_6-DMSO, or CD_3OD as solvent and Me_4Si as internal substance. IR spectra were recorded on a Nicolet Avatar 360 RT-IR spectrophotometer. Mass spectra were recorded on an Applied Bio systems MDS SCIEX 3200Q-TRAP mass spectrometry (MS) system with electro spray ionization (ESI†) and direct injection. The HRFABMS spectra were recorded on a Bruker APEX-FTMS apparatus. Elemental analysis was performed using a Vario RL analyzer. Melting points were determined on a Yanaco MP-500 melting point apparatus and are uncorrected. HPLC analysis were run on Agilent-1200 series HPLC system equipped with a photodiode array detector, using a Hypersil Gold C18 column (dimensions 250 × 4.6 mm, particle size 5 μm). Photodiode array (PDA) detector range was set as 210–600 nm.

4.2 Synthesis of oxazolidone derivatives

4.2.1 Synthesis of amides 1a, 1j, 1k, 1n, 1o and 1q–1t. Palmitoyl chloride (83 mg, 0.3 mmol) in CH_2Cl_2 (2 mL) was added dropwise to a mixture of amine (0.3 mmol) and Et_3N (0.08 mL, 0.6 mmol) in anhydrous CH_2Cl_2 (2 mL) under a nitrogen atmosphere. The resulting solution was stirred at room temperature for 4 h, then quenched with saturated aqueous

ammonium chloride, and extracted with CH_2Cl_2 (3 × 10 mL). The combined organic phases were washed with brine, dried over anhydrous Na_2SO_4, filtered, and concentrated under reduced pressure. The residue was purified by flash chromatography on silica gel and **1a**, **1j**, **1k**, **1n**, **1o** and **1q–1t** were then obtained.[21]

4.2.2 Synthesis of amides 1l and 1m. A solution of 1-(3-hydroxypyrrolidin-1-yl)hexadecan-1-one (19 mg, 0.06 mmol) in THF (1 mL) was added slowly to a suspension of NaH (60% in mineral oil, 5 mg) in anhydrous THF (5 mL), under a nitrogen atmosphere at 0 °C. After stirring at the same temperature for 5 min, a solution of CH_3I (0.15 mmol) in THF (0.5 mL) was slowly added. The reaction mixture was stirred at 0 °C for 3 h before quenched with saturated aqueous ammonium chloride (5 mL) and extracted with EtOAc (3 × 5 mL). The combined organic layers were treated using the same procedure as 2.2.1 to afford **1l** and **1m**.[23]

4.2.3 Synthesis of amides 1c and 1d. A solution of 4 M HCl (1 mmol, 0.25 mL dioxane) was added slowly to 10 mL *tert*-butyl 1-palmitoylpyrrolidin-3-ylcarbamate (60.0 mg, 0.14 mmol) methanol solution at 0 °C under a nitrogen atmosphere. The resulting solution was stirred at 0 °C for 2 h, quenched with a saturated aqueous solution of Na_2CO_3, and extracted with EtOAc (3 × 20 mL). The combined organic phases were washed with brine, dried over anhydrous Na_2SO_4, filtered, and concentrated under reduced pressure. The residue was purified by flash chromatography on silica gel (eluent : MeOH/CH_2Cl_2 = 1 : 15) to afford **1c** and **1d**.[25,26]

4.2.4 Synthesis of amides 1e and 1f. I_2 solution (76 mg, 0.3 mmol) in THF (2 mL) was added slowly to a mixture of imidazole (27 mg, 0.4 mmol) and PPh_3 (79 mg, 0.3 mmol) in THF (5 mL), under a nitrogen atmosphere at 0 °C. After stirring at the same temperature for 1 h, a THF solution (2 mL) of 1-(2-(hydroxymethyl) pyrrolidin-1-yl) hexadecan-1-one (71 mg, 0.2 mmol) was slowly added. The reaction mixture was stirred at 0 °C for 0.5 h and allowed to warm slowly to room temperature over 2 h. The reaction was quenched with a saturated solution of $Na_2S_2O_3$ and extracted with EtOAc (3 × 5 mL). The combined organic layers were dried over anhydrous Na_2SO_4, filtered, and concentrated under reduced pressure. The mixture in EtOAc (10 mL) was treated with 10% Pd/C (100 mg) and purged with H_2. After stirring for 12 h at room temperature, the reaction mixture was filtered through celite and concentrated. The residue was purified by flash chromatography on silica gel (eluent : EtOAc/PE 1 : 5) to afford **1e** and **1f**.[27,28]

4.2.5 Synthesis of oxazolidone imides 1i, 2a–2h, 3a–3d and 3h–3s. A CH_2Cl_2 (5 mL) solution of oxalyl dichloride (0.06 mL, 0.66 mmol) was added slowly to a solution of the suitable acid (0.55 mmol) and dimethylformamide (0.05 mL) under a nitrogen atmosphere at 0 °C. The reaction mixture was stirred at 0 °C for 1 h and evaporated under reduced pressure. The acid chloride obtained was used as such for the next reaction due to its high instability. A hexane solution (0.2 mL) of 2.5 Mn-BuLi (0.55 mmol, hexane) was added slowly to a THF solution (5 mL) of 2-oxazolidone (44 mg, 0.5 mmol), under a nitrogen atmosphere at −78 °C. After stirring at the same temperature for 10 min, a THF solution (2 mL) of acid chloride (0.55 mmol) was slowly added. The reaction mixture was stirred at −78 °C for 0.5 h and allowed to warm slowly to room temperature over 5 h. The reaction was quenched with saturated aqueous ammonium chloride (1.0 mL) and extracted with EtOAc (3 × 5 mL). The combined organic layers were treated using the same procedure as 2.2.1 to afford **1i**, **2a–2h**, **3a–3d** and **3h–3s**.[29]

4.2.6 Synthesis of acids 3q-1 and 3t-1. Thionyl dichloride (0.2 mL, 3 mmol) was slowly added to 10 mL CH_3OH solution of the corresponding carboxylic acid (2.0 mmol) under a nitrogen atmosphere at 0 °C. The reaction mixture was stirred at 0 °C for 2 h and evaporated under reduced pressure. The product was dissolved in acetone (15 mL) and treated with K_2CO_3 (552 mg, 4 mmol) and alkyl bromide (2.5 mmol). The reaction mixture was filtered and concentrated under reduced pressure after being refluxed for 8 h. The residue was dissolved in a 1 : 1 mixture of aqueous 2 M NaOH and MeOH (16 mL), stirred at room temperature for 4 h, then treated with 2 M HCl, and extracted with EtOAc (3 × 5 mL). The combined organic layers were dried over anhydrous Na_2SO_4, filtered, and concentrated under reduced pressure. The residue was purified by flash chromatography on silica gel to afford **3q-1** and **3t-1**.[14]

4.2.7 Synthesis of carbamates 3e–3g. A CH_2Cl_2 solution (2 mL) of bis(trichloromethyl) carbonate (98 mg, 0.33 mmol) was added dropwise to a solution of 2-oxazolidone (44 mg, 0.5 mmol) and Et_3N (0.16 mL, 1.2 mmol) in CH_2Cl_2 (5 mL) under a nitrogen atmosphere. After stirring at 0 °C for 1 h and room temperature for 2 h, the amine (0.4 mmol) in CH_2Cl_2 (1 mL) was added dropwise to the mixture under a nitrogen atmosphere. The resulting mixture was stirred at room temperature for 5 h, quenched with saturated aqueous ammonium chloride, and extracted with CH_2Cl_2 (3 × 10 mL). The combined organic phases were washed with brine, dried over anhydrous Na_2SO_4, filtered, and concentrated under reduced pressure. The residue was purified by flash chromatography on silica gel to afford **3e–3g**.[30]

4.3 *In vitro* biological evaluation of oxazolidone derivatives

4.3.1 HPLC-MS/MS analysis. A HPLC-MS/MS method was developed and validated for free fatty acids (FFAs) quantification. An ABI 3200 Q-Trap mass spectrometer equipped with Agilent 1200-HPLC system was used. FFAs were eluted at 1.0 mL min^{-1} at 40 °C with MeOH : water 95 : 5, v/v, each containing 0.25% acetic acid and 5 mmol L^{-1} ammonium acetate, pH = 7.4. The molecular ions were monitored by ESI† negative mode at m/z = 267 for heptadecenoic acid, m/z 303 for arachidonic acid, and m/z 269 for C17:0 FFAs.

4.3.2 Protein preparation and enzymatic assay. HEK293 cells overexpressing rat NAAA (HEK293-rNAAA) or rat FAAH (HEK293-rFAAH) were maintained in Dulbecco's modified Eagle medium (DMEM, Hyclone, Beijing, China) supplemented with 10% fetal bovine serum (FBS, Gibco®, Shanghai, China) containing 0.3 mg mL^{-1} geneticin G418. HEK293-rNAAA or HEK293-rFAAH cells were harvested, washed with PBS, sonicated in 20 mM Tris–HCl (pH 7.5) containing 0.32 M sucrose, and centrifuged at 800 × g for 15 min at 4 °C. The supernatants were collected, and the protein concentrations were measured

by a BCA protein assay kit (Pierce, Shanghai, China). NAAA activity was measured by incubating 30 μg recombinant rNAAA protein with 25 μM heptadecenoylethanolamide at 37 °C for 30 min in 0.2 mL of phosphate buffer (50 mM, pH 5.0) containing 0.1% Triton X-100 and 3 mM dithiothreitol with or without the tested compounds. FAAH activity was measured by incubating 30 μg of protein derived from the HEK293-rFAAH cell extract at 37 °C in Tris–HCl buffer (50 mM, pH 8.0) containing fatty acid-free bovine serum albumin (0.05%). Anandamide (25 μM) was used as the substrate for FAAH. The reactions were terminated by adding 200 μL of methanol containing 1 nmol heptadecanoic acid as internal standard, and the remaining substrates were analysed by HPLC-MS/MS. IC_{50} of each compound was analysed by GraphPad Prism 5.

4.3.3 Dialysis assay. The dialysis assay was performed using Slide-A-Lyzer dialysis cassettes (Pierce, Shanghai, China). Briefly, 2 mg of NAAA protein was incubated with **2f** or dimethyl sulfoxide (DMSO) in 4 mL of Tris–HCl buffer (50 mM, pH 5.0) for 10 min at 37 °C. The mixed reaction solution was loaded into a dialysis cartridge using a syringe and incubated in Tris–HCl buffer (50 mM, pH 5.0) at 4 °C for 8 h. The samples in the dialysis cassettes were collected for the NAAA enzymatic assay.

4.3.4 Rapid dilution assay. The rapid dilution assay was performed following a previous reported method.[21] Briefly, samples containing 100-fold concentrated rNAAA protein were pre-incubated with 10-fold of the IC_{50}-equivalent concentration of compounds or vehicle (1% DMSO) for 10 min at 37 °C. The samples were then diluted 100-fold with assay buffer containing substrate to initiate the reactions, and the time course of product formation was determined by HPLC-MS analysis.

4.4 *In vivo* anti-inflammatory and analgesic activity of compound 2f

All animal experiments were performed in accordance with 'Guide and Care and Use of Laboratory Animals' from National Institutes of Health (NIH) and approved by the Animal Care and Use Committees of Xiamen University in China.

4.4.1 *In vivo* analgesic activity of compound 2f. Formalin-induced pain model was used to evaluate the *in vivo* analgesic activity of **2f**. Male ICR mice (18–20 g) were allowed to acclimate to the Plexiglas chamber for 30 min before testing. Compound **2f** (10 mg kg^{-1}, dissolved in 5% polyethylene glycol 400 and 5% Tween-80 in saline) was then injected into the plantar surface of the right hind paw with or without PPAR-α antagonist MK886 (2 mg kg^{-1}). After 30 min, formalin (20 μL of 5% formalin, diluted in saline) was injected into the dorsal surface of the right hind paw and pain responses were recorded by an automated detecting system. The paw licking time was calculated every 5 min over the next 45 min. Nociceptive behavioural response to formalin stimulation was defined as follows: Phase I (0–10 min), acute pain response, Phase II (11–45 min), chronic pain response.

4.4.2 *In vivo* anti-inflammatory activity of compound 2f. TPA-induced ear edema model was used to test the anti-inflammatory of compound **2f**. Male WT 129s mice (20–22 g) were grouped randomly, with 8–10 animals for each group. Compound **2f** (30, 100 mg kg^{-1}) was then administered by intragastric gavage 30 min before TPA application. TPA (0.03% in acetone, 10 μL) was applied evenly to both sides of the left ear of each mouse to cause edema and inflammation, while the same amount of acetone alone was smeared to the right ear. Animals were sacrificed 3 h after treatment. Both ears were excised immediately and punched in the same position, with a diameter of 9 mm. The ear swelling was determined by weighing pieces of the ears obtained. The mRNA expression levels of TNF-α, IL-6, COX-2 and NF-κB in mice ear were determined following our previously reported method.[21]

4.4.3 Long term toxicity of compound 2f. Mice were treat with compound **2f** (100 mg kg^{-1} for 10 d, 30 mg kg^{-1} for 30 d) or indomethacin (20 mg kg^{-1} for 3 d) *via* intragastrical administration with normal diet. Mice body weight and food consumption were measured and recorded every day. The mice were sacrificed 6 h after the last administration and stomachs were harvested, rinsed with distilled water and photographed.

Acknowledgements

We thank Dr Daniele Piomelli at the University of California, Irvine for the kind gifts of the HEK293-rNAAA cells and the HEK293-rFAAH cells. YL also wants to thank William stung for English revision. This work was supported by funds from the National Natural Science Foundation of China (Grant No. 81373273 to QY and 81602974 to YL), Xiamen Southern Ocean Research Center Project (No. 14GYY018NF18) to QY, the Fundamental Research Funds for the Central Universities (No. 20720150054) to QY and China Postdoctoral Science Foundation Funded Project (No. 2016M592876XB) to YL.

References

1 K. Tsuboi, Y. X. Sun, Y. Okamoto, N. Araki, T. Tonai and N. Ueda, *J. Biol. Chem.*, 2005, **280**, 11082–11092.
2 L. Facci, R. Dal Toso, S. Romanello, A. Buriani, S. D. Skaper and A. Leon, *Proc. Natl. Acad. Sci. U. S. A.*, 1995, **92**, 3376–3380.
3 J. Lo Verme, J. Fu, G. Astarita, G. La Rana, R. Russo, A. Calignano and D. Piomelli, *Mol. Pharmacol.*, 2005, **67**, 15–19.
4 C. Solorzano, C. Zhu, N. Battista, G. Astarita, A. Lodola, S. Rivara, M. Mor, R. Russo, M. Maccarrone, F. Antonietti, A. Duranti, A. Tontini, S. Cuzzocrea, G. Tarzia and D. Piomelli, *Proc. Natl. Acad. Sci. U. S. A.*, 2009, **106**, 20966–20971.
5 S. Petrosino, T. Iuvone and V. Di Marzo, *Biochimie*, 2010, **92**, 724–727.
6 A. Calignano, G. La Rana and D. Piomelli, *Eur. J. Pharmacol*, 2001, **419**, 191–198.
7 B. Costa, S. Conti, G. Giagnoni and M. Colleoni, *Br. J. Pharmacol.*, 2002, **137**, 413–420.
8 S. Petrosino, L. Cristino, M. Karsak, E. Gaffal, N. Ueda, T. Tuting, T. Bisogno, D. De Filippis, A. D'Amico, C. Saturnino, P. Orlando, A. Zimmer, T. Iuvone and V. Di Marzo, *Allergy*, 2010, **65**, 698–711.

9 J. M. Hesselink and T. A. Hekker, *J. Pain Res.*, 2012, **5**, 437–442.
10 B. F. Cravatt, D. K. Giang, S. P. Mayfield, D. L. Boger, R. A. Lerner and N. B. Gilula, *Nature*, 1996, **384**, 83–87.
11 O. Sasso, G. Moreno-Sanz, C. Martucci, N. Realini, M. Dionisi, L. Mengatto, A. Duranti, G. Tarozzo, G. Tarzia, M. Mor, R. Bertorelli, A. Reggiani and D. Piomelli, *Pain*, 2013, **154**, 350–360.
12 J. M. West, N. Zvonok, K. M. Whitten, S. K. Vadivel, A. L. Bowman and A. Makriyannis, *PLoS One*, 2012, **7**, e43877.
13 T. Bandiera, S. Ponzano and D. Piomelli, *Pharmacol. Res.*, 2014, **86**, 11–17.
14 C. Solorzano, F. Antonietti, A. Duranti, A. Tontini, S. Rivara, A. Lodola, F. Vacondio, G. Tarzia, D. Piomelli and M. Mor, *J. Med. Chem.*, 2010, **53**, 5770–5781.
15 A. Armirotti, E. Romeo, S. Ponzano, L. Mengatto, M. Dionisi, C. Karacsonyi, F. Bertozzi, G. Garau, G. Tarozzo, A. Reggiani, T. Bandiera, G. Tarzia, M. Mor and D. Piomelli, *ACS Med. Chem. Lett.*, 2012, **3**, 422–426.
16 A. Duranti, A. Tontini, F. Antonietti, F. Vacondio, A. Fioni, C. Silva, A. Lodola, S. Rivara, C. Solorzano, D. Piomelli, G. Tarzia and M. Mor, *J. Med. Chem.*, 2012, **55**, 4824–4836.
17 S. Ponzano, F. Bertozzi, L. Mengatto, M. Dionisi, A. Armirotti, E. Romeo, A. Berteotti, C. Fiorelli, G. Tarozzo, A. Reggiani, A. Duranti, G. Tarzia, M. Mor, A. Cavalli, D. Piomelli and T. Bandiera, *J. Med. Chem.*, 2013, **56**, 6917–6934.
18 R. Vitale, G. Ottonello, R. Petracca, S. M. Bertozzi, S. Ponzano, A. Armirotti, A. Berteotti, M. Dionisi, A. Cavalli, D. Piomelli, T. Bandiera and F. Bertozzi, *ChemMedChem*, 2014, **9**, 323–336.
19 M. Migliore, S. Pontis, A. L. Fuentes de Arriba, N. Realini, E. Torrente, A. Armirotti, E. Romeo, S. Di Martino, D. Russo, D. Pizzirani, M. Summa, M. Lanfranco, G. Ottonello, P. Busquet, K. M. Jung, M. Garcia-Guzman, R. Heim, R. Scarpelli and D. Piomelli, *Angew. Chem., Int. Ed.*, 2016, **55**, 11193–11197.
20 A. Ribeiro, S. Pontis, L. Mengatto, A. Armirotti, V. Chiurchiu, V. Capurro, A. Fiasella, A. Nuzzi, E. Romeo, G. Moreno-Sanz, M. Maccarrone, A. Reggiani, G. Tarzia, M. Mor, F. Bertozzi, T. Bandiera and D. Piomelli, *ACS Chem. Biol.*, 2015, **2015**(10), 1838–1846.
21 Y. Li, L. Yang, L. Chen, C. Zhu, R. Huang, X. Zheng, Y. Qiu and J. Fu, *PLoS One*, 2012, **7**, e43023.
22 L. Yang, L. Li, L. Chen, Y. Li, H. Chen, Y. Li, G. Ji, D. Lin, Z. Liu and Y. Qiu, *Sci. Rep.*, 2015, **5**, 13565.
23 E. M. Smith, G. F. Swiss, B. R. Neustadt, E. H. Gold, J. A. Sommer, A. D. Brown, P. J. Chiu, R. Moran, E. J. Sybertz and T. Baum, *J. Med. Chem.*, 1988, **31**, 875–885.
24 C. M. Yea, C. E. Allan, D. M. Ashworth, J. Barnett, A. J. Baxter, J. D. Broadbridge, R. J. Franklin, S. L. Hampton, P. Hudson, J. A. Horton, P. D. Jenkins, A. M. Penson, G. R. Pitt, P. Riviere, P. A. Robson, D. P. Rooker, G. Semple, A. Sheppard, R. M. Haigh and M. B. Roe, *J. Med. Chem.*, 2008, **51**, 8124–8134.
25 B. J. Backes, K. Longenecker, G. L. Hamilton, K. Stewart, C. Lai, H. Kopecka, T. W. von Geldern, D. J. Madar, Z. Pei, T. H. Lubben, B. A. Zinker, Z. Tian, S. J. Ballaron, M. A. Stashko, A. K. Mika, D. W. Beno, A. J. Kempf-Grote, C. Black-Schaefer, H. L. Sham and J. M. Trevillyan, *Bioorg. Med. Chem. Lett.*, 2007, **17**, 2005–2012.
26 S. J. Macdonald, D. J. Belton, D. M. Buckley, J. E. Spooner, M. S. Anson, L. A. Harrison, K. Mills, R. J. Upton, M. D. Dowle, R. A. Smith, C. R. Molloy and C. Risley, *J. Med. Chem.*, 1998, **41**, 3919–3922.
27 I. Izquierdo, M. T. Plaza, J. A. Tamayo, F. Franco and F. Sánchez-Cantalejo, *Tetrahedron*, 2008, **64**, 4993–4998.
28 S. Mitsumori, H. Zhang, P. Ha-Yeon Cheong, K. N. Houk, F. Tanaka and C. F. Barbas 3rd, *J. Am. Chem. Soc*, 2006, **128**, 1040–1041.
29 L. Huang and W. D. Wulff, *J. Am. Chem. Soc*, 2011, **133**, 8892–8895.
30 J. T. Randolph, C. A. Flentge, P. P. Huang, D. K. Hutchinson, L. L. Klein, H. B. Lim, R. Mondal, T. Reisch, D. A. Montgomery, W. W. Jiang, S. V. Masse, L. E. Hernandez, R. F. Henry, Y. Liu, G. Koev, W. M. Kati, K. D. Stewart, D. W. Beno, A. Molla and D. J. Kempf, *J. Med. Chem.*, 2009, **52**, 3174–3183.